Preprint of

Optimal Experiments for Maximizing Coherence Transfer Between Coupled Spins

N. Khaneja, F. Kramer, S. J. Glaser

Optimal experiments for maximizing coherence transfer between coupled spins

Navin Khaneja,[*] Frank Kramer[†], Steffen J. Glaser [†]

August 2, 2004

Abstract

In spite of great advances in the theory and applications of magnetic resonance in the past 50 years, some very basic questions in spin physics have not yet been answered. In the absence of relaxation losses, what is the maximum amount of coherence that can be transfered between coupled spins under general coupling tensors in a given time and how can this be realized experimentally? Since transfer of coherence between spins forms the basis for multidimensional experiments in NMR spectroscopy, the answers to these questions are of both practical and theoretical interest. Computing the physical limits of coherence transfer involves characterizing unitary evolutions that can be synthesized in a given time. Here we derive these limits and show how they can be achieved experimentally.

1 Introduction

Computing how close a quantum mechanical system can be driven from a given initial state to a desired target state in a specified amount of time is an important practical problem. This problem arises in the areas of coherent spectroscopy and control of quantum systems where one actively manipulates quantum dynamics through electromagnetic fields of appropriate frequencies. However in most applications, external controls alone are not sufficient to bring the system to a desired target state. The evolution under the internal Hamiltonian is essential to move between quantum mechanical states of interest. For example, in NMR spectroscopy, appropriate combinations of external excitation through radio-frquency (rf) pulses and evolution under couplings between nuclear spins is used to steer a spin system to a target state, e.g. to transfer coherence from one spin to another. The necessity of having the spin system evolve under its internal Hamiltoian puts physical limits on the minimum time it takes to transfer coherence between coupled spins and on the maximum coherence that can be transferred in a specidied time.

Until now the limits of coherence transfer between coupled spins in a specified time were unknown. In this paper, we solve this problem for general coupling tensors and find the optimal pulse sequence for achieving the optimal coherence transfer. Computing such bounds and the optimal pulse sequences involves explicit characterization of the set of unitary propagators that can be synthesized in a given time. In our recent work on time-optimal control of spin systems [1, 2], we presented an explicit characterization of all the unitary transformations that can be produced in a coupled spin system in a specified time. Here we use these methods to compute the maximum coherence transfer efficiency between coupled spins in a specified time. We also provide experimental data which shows how these methods can be used to improve sensitivity of current NMR experiments when the time for coherent evolution is restricted. Finally we discuss how these methods might be generalized to larger spin systems and other applications involving control of quantum dynamics.

2 Theory

We consider a pair of coupled spins, where the coupling Hamiltonian $\mathcal{H}_c$ has the form

$$\mathcal{H}_c = 2\pi C(\mu_1 I_x S_x + \mu_2 I_y S_y + \mu_3 I_z S_z), \tag{1}$$

where in the following we assume $|\mu_3| \geq |\mu_2| \geq |\mu_1|$.

2

Note that the above form of the coupling Hamiltonian is completely general as any coupling term of the form

$$\mathcal{H}_c = \sum_{\alpha,\beta} C_{\alpha\beta} I_\alpha S_\beta = \mathbf{I} \, \mathbf{C} \, \mathbf{S}$$

with the general coupling tensor

$$\mathbf{C} = \begin{pmatrix} C_{xx} & C_{xy} & C_{xz} \\ C_{yx} & C_{yy} & C_{yz} \\ C_{zx} & C_{zy} & C_{zz} \end{pmatrix}$$

with arbitrary real elements C_{ij} can be transformed to the form given in Eq. 1 by local unitary transformations on the two spins [2]. To see this, observe that by *singular value decomposition* $\mathbf{C}$ can be written as

$$\mathbf{C} = \Theta_1 \begin{bmatrix} \mu_1 & 0 & 0 \\ 0 & \mu_2 & 0 \\ 0 & 0 & \mu_3 \end{bmatrix} \Theta_2,$$

where Θ_1 and Θ_2 are three-dimensional rotations. By local unitary transformations we can transform the coupling tensor $\mathbf{C} \to U\mathbf{C}V$ where U, V are three dimensional rotations with positive determinant, reflecting rotations on spin I and S respectively. Therefore U and V can be chosen so that

$$U\mathbf{C}V = \pm \begin{bmatrix} \mu_1 & 0 & 0 \\ 0 & \mu_2 & 0 \\ 0 & 0 & \mu_3 \end{bmatrix}.$$

We assume that the two spins under consideration can be selectively manipulated at rates faster than the coupling evolution, which is always possible if the frequency difference between the spins which is much larger than the strength of coupling Hamiltonian. This allows us to produce any local unitary transformation in a time during which there is negligible evolution under the coupling Hamiltonian. Under these assumptions, we can completely characterize all the unitary transformations that can be achieved in time t. The results derived in this paper use the following theorem which characterizes the unitary transformations that can be achieved in any given time t [1, 2].

Theorem 1:[2] Given the coupling Hamiltonian $\mathcal{H}_c = 2\pi C(\mu_1 I_x S_x + \mu_2 I_y S_y + \mu_3 I_z S_z)$ for a two spin system, all unitary transformations that can be synthesized in time t have the form

$$U(t) = K_1 A(t) K_2, \tag{2}$$

where $A(t)$ denotes the nonlocal unitary transformation $\exp\{-\mathrm{i}2\pi Ct(\alpha I_x S_x + \beta I_y S_y + \gamma I_z S_z)\}$. Here the vector (α, β, γ) lies in the convex cone generated by vectors (μ_1, μ_2, μ_3), $(\mu_1, -\mu_2, -\mu_3)$, $(-\mu_1, -\mu_2, \mu_3)$, $(-\mu_1, \mu_2, -\mu_3)$ and their various permutations (e.g. (μ_1, μ_3, μ_2) is a permutation of (μ_1, μ_2, μ_3)). K_1 and K_2 are local unitary transformations. A vector x belongs to the cone of vectors $\{y_i\}$ if $x = \sum_i \alpha_i y_i$, where $\alpha_i \geq 0$ and $\sum_i \alpha_i \leq 1$.

It is straightforward to see that any unitary transformation in Eq. (2) can be achieved in time t. Starting from the Hamiltonian of the form $\mu_1 I_x S_x + \mu_2 I_y S_y + \mu_3 I_z S_z$, by double 90°_y rotations on both spins, we can prepare the effective Hamiltonian $\mu_3 I_x S_x + \mu_2 I_y S_y + \mu_1 I_z S_z$. Similarly, by selective 180°_x rotations on one of the spins, we can also prepare the effective Hamiltonian $\mu_1 I_x S_x - \mu_2 I_y S_y - \mu_3 I_z S_z$. Now it is clear that by a series of such double and selective rotations any Hamiltonian of the form $p I_x S_x + q I_y S_y + r I_z S_z$ where (p, q, r) is one of (μ_1, μ_2, μ_3), $(\mu_1, -\mu_2, -\mu_3)$, $(-\mu_1, -\mu_2, \mu_3)$, $(-\mu_1, \mu_2, -\mu_3)$ or their permutations can be synthesized. Since all these Hamiltonians commute, we can, by concatenation of evolution under these transformed Hamiltonians, synthesize an average Hamiltonian $\alpha I_x S_x + \beta I_y S_y + \gamma I_z S_z$, where (α, β, γ) lies in the specified convex cone. Since local unitary transformations are assumed to take neglible time to produce, it is now clear that any U as defined in Eq. (2) can be synthesized. Using some important convexity results in matrix analysis, it can be shown that these are the only unitary evolutions that can be synthesize in time t [2].

Table 1: Maximum transfer efficiency $\eta^*(t)$ and minimum time $t_{\min}$ for complete transfer

Transfer	$\eta^*(t)$	$t_{\min}^{-1}$
$I_x \to S_x$	$\sin^2(\frac{\pi}{2} C(|\mu_3| + |\mu_2|)t)$	$C(|\mu_3| + |\mu_2|)$
$I^- \to S^-$	$\sin(\pi C a) \sin(\pi C b)$	$\frac{2}{3} C(|\mu_3| + |\mu_2| + |\mu_1|)$
$I_x \to 2 I_z S_x$	$\sin(\pi C |\mu_3| t)$	$2 C |\mu_3|$
$I^- \to 2 I_z S^-$	$\max_x \ \sin(\frac{\pi}{2} C\{|\mu_3| + |\mu_2| - |\mu_1| + x\}t) \cos(\pi C t x)$	$C(|\mu_3| + |\mu_2| - |\mu_1|)$
$I_x S_\beta \to I_\beta S_x$	$\sin(\frac{\pi}{2} C(|\mu_3| + |\mu_2|)t)$	$C(|\mu_3| + |\mu_2|)$
$I^- S_\beta \to I_\beta S^-$	$\sin(\frac{\pi}{2} C(|\mu_3| + |\mu_2|)t)$	$C(|\mu_3| + |\mu_2|)$

Note: $I^- = I_x - \mathrm{i} I_y$ and $I_\beta = \frac{1}{2} - I_z$. For the transfer $I^- \to S^-$, the optimal values of a and b are completely characterized by the two conditions $a + 2b = (|\mu_3| + |\mu_2| + |\mu_1|)\, t$ and $\tan(\pi C a) = 2 \tan(\pi C b)$.

4

We now use this result to compute the maximum coherence that can be transferred between coupled spins in a specified time t. Let the initial density operator terms of interest be $\rho(0)$ and denote the density operator at time t by $\rho(t) = U(t)\rho(0)U(t)^\dagger$. The efficiency of transfer to a target operator F at time t is defined as [3]

$$\eta(t) = \frac{|\mathrm{tr}(F^\dagger \rho(t))|}{\|F\| \, \|\rho(0)\|}. \tag{3}$$

Result 1: Given the coupling Hamiltonian $\mathcal{H}_c = 2\pi C(\mu_1 I_x S_x + \mu_2 I_y S_y + \mu_3 I_z S_z)$, the maximum efficiency $\eta^*(t)$ of the coherence transfer in time t and the minimum time $t_{\min}$ for complete transfer for important experiments are summarized in Table 1.

The plot of the maximum achievable efficiency η^* versus the mixing time t also gives us the minimum time it takes to achieve a desired coherence transfer efficiency. We will refer to this plot as TOP (time-optimal pulse) curve. In Table 1, complete characterizations of TOP curves $\eta^*(t)$ are given for widely used coherence transfer elements, such as Cartesian in-phase to in-phase transfer ($I_x \rightarrow S_x$) as in refocussed INEPT [4], coherence-order-selective in-phase to in-phase transfer ($I^- \rightarrow S^-$) as in sensitivitiy enhanced ICOS-CT experiments [5], Cartesian in-phase to antiphase transfer ($I_x \rightarrow 2I_z S_x$) as in standard INEPT [6], coherence-order-selective in-phase to antiphase transfer ($I^- \rightarrow 2I_z S^-$) as in sensitivity enhanced COS-CT [7], and line-selective to line-selective transfer $I_x S_\beta \rightarrow I_\beta S_x$ and $I^- S_\beta \rightarrow I_\beta S^-$ as in TROSY [8, 9]. Note that by fast local unitary transformations I_x can be rapidly flipped to I_y or I_z, $I^- = I_x - iI_y$ can be transformed to $I^+ = I_x + iI_y$, and $I_\beta = \frac{1}{2} - I_z$ can be transformed to $I_\alpha = \frac{1}{2} + I_z$ and vice versa. Hence, each of the specific transfers stated in Table represents a whole class of locally equivalent transfers with the same TOP curves $\eta^*(t)$ and the same minimum time $t_{\min}$ to achieve complete transfer.

Examples of TOP curves are presented in Fig. 1 for four characteristic coupling tensors. Fig. 1 A corresponds to the case of longitudinal, Ising-type coupling with $(\mu_1, \mu_2, \mu_3) = (0, 0, 1)$, which is characteristic for heteronuclear experiments [10, 11]. Fig. 1 B shows the cae of planar coupling [12], also known as XY model [13] with $(\mu_1, \mu_2, \mu_3) = (0, 1, 1)$. Fig. 1 C represents the generic case of homonuclear J coupling in isotropic solutions, also known as Heisenberg coupling with $(\mu_1, \mu_2, \mu_3) = (1, 1, 1)$. Finally, Fig. 1 D corresponds to the case of dipolar coupling with $(\mu_1, \mu_2, \mu_3) = (-0.5, -0.5, 1)$, which is the dominant homonuclear coupling term in solid state NMR and also important in anisotripic solutions [14]. For example, in the case of the Cartesian transfer $I_x \rightarrow S_x$ under dipolar coupling (red TOP curve in Fig. 1 D), the minimum time to achieve full transfer is 2/(3 C)=0.66/C. In contrast,

5

conventional pulse sequences [4, 15] based solely on non-selective rf pulses require a 50% longer trans-fer time t. From Table 1 it is follows that $t_{\min}(I_x \to S_x) = t_{\min}(I_x S_\beta \to I_\beta S_x) = t_{\min}(I^- S_\beta \to I_\beta S^-)$ and

$$ t_{\min}(I_x \to 2I_z S_x) \leq t_{\min}(I_x \to S_x) \leq t_{\min}(I^- \to 2I_z S^-) \leq t_{\min}(I^- \to S^-) $$

if $|\mu_2| + |\mu_3| \geq 5|\mu_1|$ (c.f. Fig. 1 A, B), else (c.f. Fig. 1 C, D)

$$ t_{\min}(I_x \to 2I_z S_x) \leq t_{\min}(I_x \to S_x) \leq t_{\min}(I^- \to S^-) \leq t_{\min}(I^- \to 2I_z S^-). $$
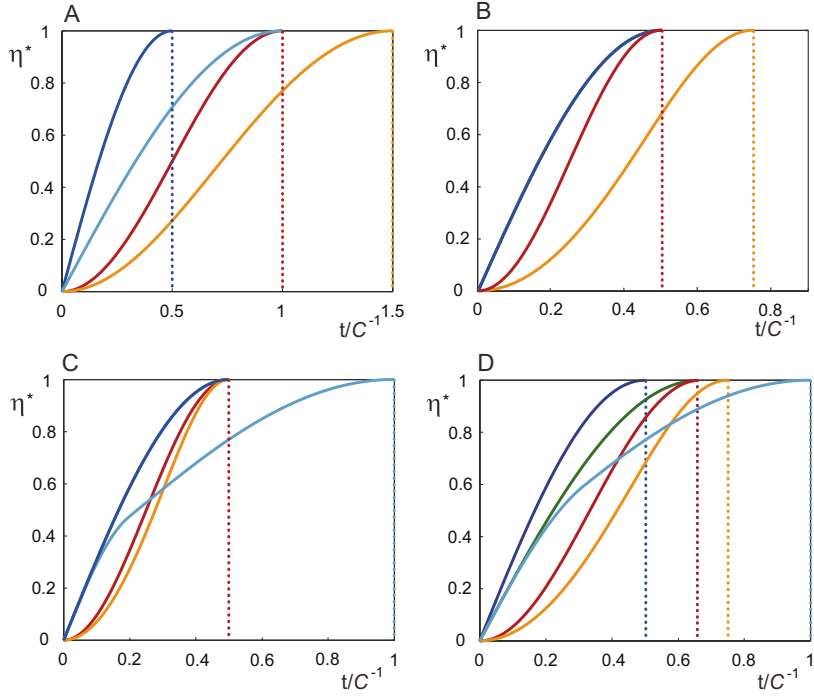

Figure 1: Graphical representations of the TOP (time-optimal pulse) curves $\eta^*(t)$ for characteristic coherence transfers under (A) longitudinal (Ising) coupling with $(\mu_1, \mu_2, \mu_3) = (0, 0, 1)$, (B) planar coupling with $(\mu_1, \mu_2, \mu_3) = (0, 1, 1)$, (C) isotropic (Heisenberg) coupling with $(\mu_1, \mu_2, \mu_3) = (1, 1, 1)$, and (D) dipolar coupling with $(\mu_1, \mu_2, \mu_3) = (-0.5, -0.5, 1)$. The curves represent the transfers $I_x \to S_x$ (red), $I^- \to S^-$ (orange), $I_x \to 2I_z S_x$ (dark blue), $I^- \to 2I_z S^-$ (light blue), $I_x S_\beta \to I_\beta S_x$ and $I^- S_\beta \to I_\beta S^-$ (green). Dark blue curves are overlapping with green curves in (A), (B), and (C), and with the light blue curve in (B). The dotted vertical lines indicate the minimum time $t_{\min}$ to achieve full transfers.

In Fig. 1 C and D, the characteristic shape of the light blue TOP curves for the transfer $I^- \to 2I_z S^-$ results from the need to refocus the $I_z S_z$ part of the coupling term, for details see *supporting methods*. Schematic representation of time optimal pulse sequences achieving the transfer limits are shown in Fig. 2.

The proof of the optimal transfer efficiencies $\eta^*(t)$ and minimum times $t_{\min}$ summarized in Table 1 uses the characterization of all the unitary transformations that can be achieved in a given time t as characterized in Eq. (2), for details see *supporting methods*. Here, we illustrate the basic ideas involved in proving the above relations by considering the first example $(I_x \rightarrow S_x)$. For this case, Eq. (3) reduces to

$$\eta(t) = |\mathrm{tr}\{S_x U(t) I_x U^\dagger(t)\}| \tag{4}$$

as $\|I_x\| = \|S_x\| = 1$. We need to find the unitary propagator $U(t)$ that maximizes $\eta(t)$. As explained before, it takes negligible time to synthesize the local unitary transformations K_1 and K_2 in Eq. (2). Let $K_2 I_x K_2^\dagger = m_1 I_x + m_2 I_y + m_3 I_z$ and $K_1^\dagger S_x K_1 = n_1 S_x + n_2 S_y + n_3 S_z$, where $\sum_i m_i^2 = 1$ and
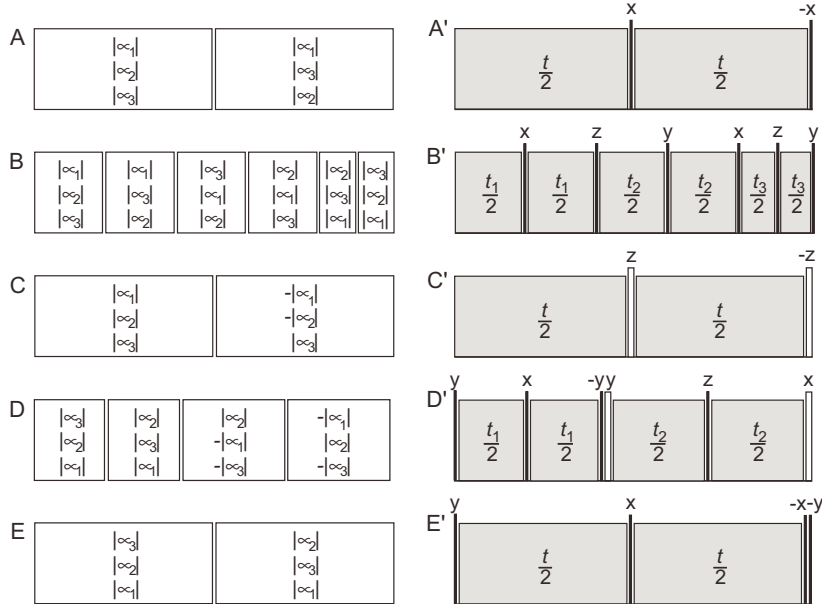

Figure 2: Schematic representation of time optimal pulse (TOP) sequences achieving the physical limit of transfer efficiency $\eta^*(t)$ in a given time t for the transfers $I_x \rightarrow S_x$ (A, A′), $I^- \rightarrow S^-$ (B, B′), $I_x \rightarrow 2I_z S_x$ (C, C′), $I^- \rightarrow 2I_z S^-$ (D, D′), $I_x S_\beta \rightarrow I_\beta S_x$ and $I^- S_\beta \rightarrow I_\beta S^-$ (E, E′). Panels A-E show the sequence of effective coupling Hamiltonians to be created during the sequence, where the tripple in each box represents the prefactors of the bilinear coupling terms $2\pi C I_x S_x$, $2\pi C I_y S_y$, and $2\pi C I_z S_z$ in a toggling frame, respectively. For simplicity, here it is assumed that the initial coupling Hamiltonian H_c can be transformed by selective 180° rotations on the spins to $+2\pi C(|\mu_1| I_x S_x + |\mu_2| I_y S_y + |\mu_3| I_z S_z)$. Panels A′-E′ show schematic pulse sequences, where the gray boxes represent pulse sequence elements creating the effective Hamitonian $2\pi C(|\mu_1| I_x S_x + |\mu_2| I_y S_y + |\mu_3| I_z S_z)$ (or $-2\pi C(|\mu_1| I_x S_x + |\mu_2| I_y S_y + |\mu_3| I_z S_z)$). The optimal durations t_1, t_2, and t_3 in B′ and of t_1 and t_2 in D′ are specified in the *supplementary methods*. Narrow and wide bars represent 90° and 180° pulses, respectively. Solid bars represent nonselective pulses and open bars represent spin-selective pulses.

$\sum_j n_j^2 = 1$. Eq. (4) then can be written as

$$\eta(t) = m_1 n_1 \sin(\pi C\beta t)\sin(\pi C\gamma t) + m_2 n_2 \sin(\pi C\alpha t)\sin(\pi C\gamma t) + m_3 n_3 \sin(\pi C\alpha t)\sin(\pi C\beta t), \quad (5)$$

where (α, β, γ) lies in the convex cone generated by vectors (μ_1, μ_2, μ_3), $(\mu_1, -\mu_2, -\mu_3)$, $(-\mu_1, -\mu_2, \mu_3)$, $(-\mu_1, \mu_2, -\mu_3)$ and their various permutations. If $\beta + \gamma$ is fixed then $\sin(\pi C\beta t)\sin(\pi C\gamma t)$ achieves it maximum value at $\beta = \gamma$. Given the restrictions on (α, β, γ) as described above, this maximum value is achieved when $\beta + \gamma = |\mu_2| + |\mu_3|$ and the maximum value is $\sin^2(\frac{\pi}{2}C(|\mu_3| + |\mu_2|)t)$ (c.f. red curves in Fig. 1). Therefore Eq. (5) is maximized for $m_1 = n_1 = 1$ and for $\beta = \gamma = \frac{1}{2}(|\mu_3| + |\mu_2|)$. Thus the largest value of Eq. (5) is 1 and is achieved at $t_{\min} = \{C(|\mu_3| + |\mu_2|)\}^{-1}$. The initial coupling Hailtonain H_c can be transformed by selective 180° rotations on the spins to either $2\pi C(|\mu_1|I_xS_x + |\mu_2|I_yS_y + |\mu_3|I_zS_z)$ or $-2\pi C(|\mu_1|I_xS_x + |\mu_2|I_yS_y + |\mu_3|I_zS_z)$. The maximum efficiency can be achieved by evolution under the Hamiltonian $\pm 2\pi C(|\mu_1|I_xS_x + |\mu_2|I_yS_y + |\mu_3|I_zS_z)$ for a duration $\frac{t}{2}$ followed by evolution under $\pm 2\pi C(|\mu_1|I_xS_x + |\mu_3|I_yS_y + |\mu_2|I_zS_z)$ for another period $\frac{t}{2}$, as depicted in Fig. 2 A, A′.

3   Experimental

For practical NMR applications, the required selective manipulations of spins are most straigtforward to implement in heteronuclear spin systems, which implies the weak coupling (Ising coupling). For homonuclear spin systems with general coupling tensors, rapid selective manipulation of spins is possible if the resonance frequencies of the spins of interest are well separated. The physical limits of coherence transfer efficiency in a given time will motivate the development of pulse sequence elements (represented by boxes in Fig. 2 A′-E′) for suppressing chemical shifts for given frequency ranges of practical interest to approach an effective coupling Hamiltonian of the form $\pm 2\pi C(|\mu_1|I_xS_x + |\mu_3|I_yS_y + |\mu_2|I_zS_z)$, as required by the time-optimal pulse sequences (c.f. gray boxes in Fig. 2 A′-E′).

In order to experimentally demonstrate an example of a nontrivial optimal coherence transfer sequence, we implemented the transfer $I^- \to S^-$ for an effective Hamiltonian of the form given in Eq. (1) with $C = 10.8$ Hz and $(\mu_1, \mu_2, \mu_3) = (0.03, 0.88, 0.88)$. Spins I and S were represented by the H5 and H6 proton spins of cytosine in an anisotropic solvent consisting of filamentous Pf1 phage in 90% H_2O and 10% D_2O [15, 16]. The phage concentration was adjusted such that the residual dipolar coupling constant D between I and S was the negative of the scalar coupling constant $J =$

7.2 Hz. At a magnetic field of 14.1 Tesla, the transmitter frequency was set in the center of the two resonances, resulting in offset frequencies $\nu_I = 459$ Hz and $\nu_S = -459$ Hz with a free evolution Hamiltonian of the form

$$\mathcal{H} = 2\pi\nu_I \ (I_x - S_x) + 2\pi C \ (I_y S_y + I_z S_z)$$

with $C = J - D/2 = 10.8$ Hz, where we have labeled the axes such that the convention $|\mu_3| \geq |\mu_2| \geq |\mu_1|$ is fulfilled (c.f. Eq. 1). In order to eliminate the offset terms, we used a modified Carr-Purcel sequence [17, 18, 19] with a rf amplitude $-\gamma B_1/(2\pi)$ of 31.2 kHz and delays Δ of 264 μs which results in an effective Hamiltonian

$$\mathcal{H}_{\text{eff}} = 2\pi C \ (0.03 \ I_x S_x + 0.88 \ I_y S_y + 0.88 \ I_z S_z).$$

Given this effective Hamiltonian, the optimal pulse sequence for the transfer $I^- \rightarrow S^-$ was implemented. According to Table 1, the minimum time to achieve full transfer ($\eta = 1$) is given by $t_{\min} = 3\{2C(|\mu_3| + |\mu_2| + |\mu_1|)\}^{-1} = 77.6$ ms and for a given total transfer time $t \leq t_{\min}$, the maximum possible transfer efficiency $\eta^*(t)$ is given by

$$\eta^*(t) = \sin(\pi C a) \sin(\pi C b) \tag{6}$$

(c.f. solid curve in Fig. 3A) with $(a + 2b)/t = |\mu_3| + |\mu_2| + |\mu_1| = 1.79$ and $\tan(\pi C a) = 2\tan(\pi C b)$.

In the general case where $\mu_1 \neq \mu_2 \neq \mu_3$, the optimal sequence of toggling frame Hamiltonians shown in Fig. 2 B consists of six periods which can be realized by the pulse sequence given in Fig. 2 B$'$. In the present case where $\mu_2 = \mu_3$, the general sequence of toggling frame Hamiltonians reduces to only three distinct periods with $\pm 2\pi C(|\mu_1|I_x S_x + |\mu_2|I_y S_y + |\mu_3|I_z S_z)$ for time t_1, $\pm 2\pi C(|\mu_3|I_x S_x + |\mu_1|I_y S_y + |\mu_2|I_z S_z)$ for time t_2, and $\pm 2\pi C(|\mu_2|I_x S_x + |\mu_3|I_y S_y + |\mu_1|I_z S_z)$ for time t_3. The corresponding pulse sequence can be simplified to t_1 - (90_z°) - t_2 - ($90_{-z}^\circ 90_y^\circ$) - t_3 - (90_{-y}°). (Note that due to the definition of the frame of reference, such that $|\mu_3| \geq |\mu_2| \geq |\mu_1|$ c.f. Eq. 1), the 90_y° and 90_z° pulses correspond to 90_x° and 90_y° pulses in the usual rotating frame of reference.) For any total time $t \leq t_{\min}$, the optimal durations $t_1 = t_2$ and t_3 are determined uniquely by the conditions $t_1 + t_2 + t_3 = t$ and $\tan(\pi C a) = 2\tan(\pi C b)$, where $a = (|\mu_2| + |\mu_3|)t_2 + |\mu_1|t_3$ and $b = |\mu_1|t_1 + (|\mu_2| + |\mu_3|)(t_2 + t_3)/2$ (c.f. solid curves in Fig. 3 B and *supporting methods*).

In order to record experimental transfer efficiecy curves $\eta(t)$ for the transfer $I^- \rightarrow S^-$ in the rotating frame, the intial density operator $\rho_\circ = I_x$ was prepared by selectively saturating spin S and by applying a hard 90_y° pulse to the thermal equilibrium spin I polarization. The solvent signal (H_2O) was suppressed by a combination of presaturation and pulsed field gradients. Before application of

the transfer sequence, I_x was dephased by a pulsed field gradient. After the actual coherence transfer step, a refocussing gradient of opposite sign was applied and the free induction decay was recorded. As only -1 quantum coherence is detected by the standard quadrature detection scheme, the integrated intensity of the S resonance corresponds to the experimental transfer amplitude for $I^- \to S^-$. Fig. 3 A shows the theoretical (solid line) and experimental (solid circles) transfer efficiency of the optimal pulse sequence as a function of t. For comparison, the dotted curve and open circles shows the theoretical and experimental transfer efficiency

$$\eta^{IM}(t) = \sin^2(\pi C\{|\mu_1| + |\mu_2| + |\mu_3|\}t/3)$$

of an isotropic mixing sequence with $t_1 = t_2 = t_3 = t/3$ [5, 20, 21, 22]. In the limit of short transfer times, the optimal mixing sequence provides a gain of more than 11% compared to isotropic mixing. As the transfer time t is nearing $t_{\min}$, the optimal transfer sequence approaches the isotropic mixing sequence with $t_i = t/3$ (c.f. Fig. 3 B).

4 Conclusion

If no constraint is placed on the mixing time, the maximum achievable efficiency and pulse designs for the transfers considered in this paper are well known [3, 23, 24]. However, we for the first time derive physical limits on the efficiency of coherence transfer between coupled spins 1/2 under general coupling tensors for arbitrary mixing times t. Furthermore, we give explicit shortest pulse sequences which achieve this maximum efficiency. The solution of this problem, besides being of fundamental interest in magnetic resonance, gives the best experimental designs for multidimensional NMR experiments where mixing times have to be curtailed due to relaxation losses. It is important to note that we have made no attempts in this paper to exploit the structure of relaxation. In our recent work, we have shown that in the presence of differential relaxation rates, it is possible to increase coherence transfer efficiency over one obtained by just reducing the mixing time [25, 26, 27]. However, in many practical applications, no differential relaxation exists or limited information about relaxation is available. With the development of new methods which give unitary bounds on coherence transfer efficiencies in multiple spin topologies [3, 23], it is of interest to extend the results of this paper to compute the minimum time and the corresponding pulse sequences to achieve these bounds in larger spin systems. For example, these include general I_nS spin systems (e.g. methylene or methyl groups
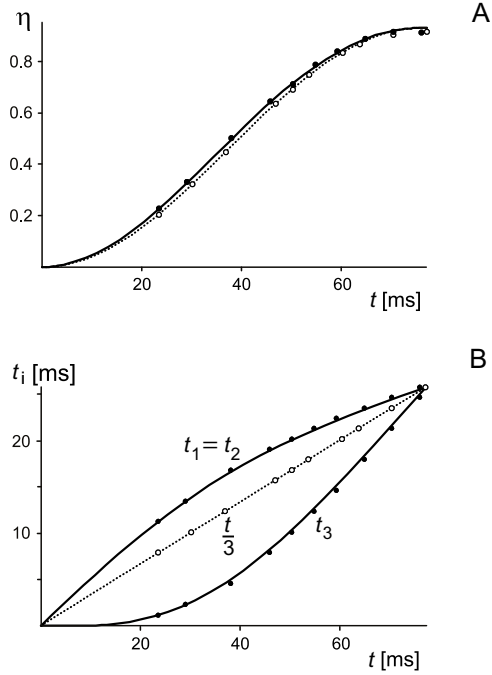
Figure 3: (A) Comparison of transfer efficiencies $\eta(T)$ for the in-phase coherence-order selective coherence transfer $I^- \to S^-$. Solid curve and black circles correspond to the theoretical (c.f. Eq. 6) and experimental transfer efficiency of the optimal pulse sequence for a non-isotropic effective Hamiltonian of the form $\mathcal{H}_{\text{eff}} = 2\pi \ 10.8 \ \text{Hz} \ (0.03 \ I_x S_x + 0.88 \ I_y S_y + 0.88 \ I_z S_z)$ as a function of the total transfer time t. The dottet curve and open circles represent the case of isotropic mixing. In order to take into account small experimental relaxation losses, the theoretical curves were multiplied by an exponential damping function $\exp\{-t/T_d\}$ with $T_d = 1.06$ s. (B) Optimal durations t_1, t_2, and t_3 (solid curves) and the durations $t_1 = t_2 = t_3 = t/3$ of an isotropic mixing sequence. The black dots correspond to actual mixing periods t_i used in the experiments, where the time resolution was limited to multiples of 1.12 ms, corresponding to a single XY-4 cycle [17], i.e. one fourth of complete a complete XY-16 cycle [18].

in side chains of proteins) and chains of coupled heteronuclear or homonuclear spins (e.g. in protein backbone or side chain experiments). The techniques presented in this paper for computing limits of coherence transfer efficiency by first characterizing the set of unitary transformations that can be synthesized in a specified time forms a systematic methodoloy for approaching these problems. Furthermore, such a characterization of unitary evolutions is of great significance in the general area of quantum information processing. This allows to address problems like characterizing the difficulty of generating a desired state in coupled spin topologies or finding the minimum time to transfer an unknown state completely between two coupled spins under a given coupling tensor.

11

1. First we consider the transfer

$$I_x \rightarrow 2I_z S_x.$$

Observe the efficiency of this transfer is the same as that of the transfer $I_x \rightarrow 2I_y S_z$, as a local rotation on spin I and S is sufficient to go between the operators $2I_y S_z$ and $2I_z S_x$. This local transformation is assumed to take negligible time. We now compute the unitary evolution $U(t)$ that maximizes $|\text{tr}(\ 2I_y S_z \ U(t)I_x U^\dagger(t))|$. Based on the characterization of $U(t) = K_1 A(t) K_2$ as in equation (2), consider the case when K_2 is identity. In this case

$$A(t)I_x A^\dagger(t) = \sin(\pi C\gamma t)\cos(\pi C\beta t) \ 2I_y S_z + \sin(\pi C\gamma t)\sin(\pi C\beta t) \ S_x$$

The maximum projecion of $K_1 A(t) I_x A^\dagger(t) K_1^\dagger$ onto $2I_y S_z$ is then $\sin(\pi C\gamma t)\cos(\pi C\beta t)$ and is achieved when K_1 is an identity transformation. This value $\sin(\pi C\gamma t)\cos(\pi C\beta t)$ is maximized for $\beta = 0$ and γt as large as possible (as long as $\gamma t \leq \frac{1}{2\pi C}$). From (2), the vector (α, β, γ) lies in the convex cone generated by vectors (μ_1, μ_2, μ_3), $(\mu_1, -\mu_2, -\mu_3)$, $(-\mu_1, -\mu_2, \mu_3)$, $(-\mu_1, \mu_2, -\mu_3)$ and their various permutations. Under these constraints the optimal values of γ and β are $|\mu_3|$ and 0 respectively. The maximum efficiency is $\sin(\pi C|\mu_3|t)$. For the local unitary transformation K_2 other than identity $K_2 I_x K_2^\dagger = m_1 I_x + m_2 I_y + m_3 I_z$, where $\sum_i m_i^2 = 1$. Each of these single spin operators have the maximum transfer efficiency of $\sin(\pi C|\mu_3|t)$ to the target state $2I_y S_z$ by choice of suitable $A(t)$ and K_1 as described above. There is no gain by having K_2 other than identity and so we achieve the maximum efficiency when $K_2 = 1$. The maximum efficiency can be achieved by evolution under the Hamiltonian $\pm 2\pi C(|\mu_1|I_x S_x + |\mu_2|I_y S_y + |\mu_3|I_z S_z)$ for $\frac{t}{2}$ amount of time followed by evolution under $\pm 2\pi C(-|\mu_1|I_x S_x - |\mu_2|I_y S_y + |\mu_3|I_z S_z)$ for another $\frac{t}{2}$ as depicted in Figure.

2. Now we consider the trasfer

$$I^- \rightarrow S^-.$$

To derive the optimal efficiency for this transfer, we state two lemmas that we will use in the course of the proof.

Lemma 1 *Let* $p = \begin{bmatrix} 1 \\ -i \\ 0 \end{bmatrix}$,

$$\Sigma = \begin{bmatrix} a_1 & 0 & 0 \\ 0 & a_2 & 0 \\ 0 & 0 & a_3 \end{bmatrix},$$

$a_i \geq 0$ and U, V, three dimensional rotation matrices. The maximum value of $\|p^\dagger U \Sigma V p\|$ is the sum of the largest two entries of a_i.

Proof: Let

$$\Lambda = \begin{bmatrix} \sqrt{a_1} & 0 & 0 \\ 0 & \sqrt{a_2} & 0 \\ 0 & 0 & \sqrt{a_3} \end{bmatrix}.$$

By definition $\Sigma = \Lambda^\dagger \Lambda$. Using Cauchy Schwartz inequality $\|p^\dagger U \Sigma V p\| \leq \|\Lambda V p\| \, \|\Lambda U p\|$. Observe, the maximum value of $\|\Lambda V p\|$ is $\sqrt{a_k + a_l}$, where a_k and a_l are the two largest diagonal entries of Σ. Therefore $\|p^\dagger U \Sigma V p\| \leq a_k + a_l$. For appropriate choice of U and V, this upper bound is achieved (For example, in case $a_1 \geq a_2 \geq a_3$, the bound is achieved for U and V identity). **Q.E.D**.

Lemma 2 Consider the function $f(\gamma, \beta, \alpha) = \sin(C\pi\gamma t) \sin(C\pi\beta t) + \sin(C\pi\gamma t) \sin(C\pi\alpha t)$, where $\gamma, \beta, \alpha \geq 0$. For a fixed value of $\gamma + \beta + \alpha$, the maximum value of $f(\gamma, \beta, \alpha)$ is $2 \sin(C\pi a) \sin(C\pi b)$, where $a + 2b = (\alpha + \beta + \gamma)t$ and $\tan(C\pi a) = 2\tan(C\pi b)$. The maximum is achieved when $\alpha = \beta$.

This is a constrained optimization problem, which can be solved by introducing the Lagrange multiplier λ and maximizing

$$\sin(C\pi\gamma t) \sin(C\pi\beta t) + \sin(C\pi\gamma t) \sin(C\pi\alpha t) + \lambda(\gamma + \beta + \alpha).$$

The computations are straightforward and have been ommitted.

We now seek to maximize the expression $\|\mathrm{tr}(S^+ U(t) I^- U^\dagger(t))\|$. Let $\mathfrak{s}$ denote the subspace spanned by the orthonormal basis $\{S_x, S_y, S_z\}$ and $\mathfrak{i}$ denote the subspace spanned by the orthonormal basis $\{I_x, I_y, I_z\}$. We represent the starting operator $\frac{1}{\sqrt{2}}(I_x - iI_y)$ as a column vector $p = \frac{1}{\sqrt{2}}[1 \ -i \ 0]^T$ in $\mathfrak{i}$. The action $I^{-1} \rightarrow K_1 I^{-1} K_1^\dagger$ can then be represented as $p \rightarrow Vp$ where V is an orthogonal matrix. Similarly the operator $S^+ = \frac{(S_x + iS_y)}{\sqrt{2}}$ is represented as a column vector $\frac{1}{\sqrt{2}}[1 \ i \ 0]^T$ in $\mathfrak{s}$. Using the charactrization of $U(t) = K_1 A(t) K_2$ in equation 2, we observe that $\|\mathrm{tr}(S^+ U(t) I^- U^\dagger(t))\|$ can be written as $\|p^\dagger U \Sigma V p\|$, where U and V are real orthogonal matrices and

$$\Sigma = \begin{bmatrix} \sin(C\pi\gamma t) \sin(C\pi\beta t) & 0 & 0 \\ 0 & \sin(C\pi\gamma t) \sin(C\pi\alpha t) & 0 \\ 0 & 0 & \sin(C\pi\alpha t) \sin(C\pi\beta t) \end{bmatrix},$$

where $\alpha + \beta + \gamma = (|\mu_1| + |\mu_2| + |\mu_3|)t$. Now using Lemma 1 and 2 we obtain that the maximum efficiency is given by $\sin(\pi C m) \sin(\pi C n)$ where $m + 2n = (|\mu_1| + |\mu_2| + |\mu_3|)t$ and $\frac{tan(\pi C m)}{tan(\pi C n)} = 2$.

In practice we can achieve this efficiency by evolving the Hamiltonian $\pm 2\pi C(|\mu_1|I_xS_x +$ $|\mu_2|I_yS_y+|\mu_3|I_zS_z)$, followed by the Hamiltonian $\pm 2\pi C(|\mu_1|I_xS_x+|\mu_3|I_yS_y+|\mu_2|I_zS_z)$ each for time $t_1/2$. This is followed by evolution of Hamiltonians $\pm 2\pi C(|\mu_3|I_xS_x+|\mu_1|I_yS_y+|\mu_2|I_zS_z)$, $\pm 2\pi C(|\mu_2|I_xS_x + |\mu_1|I_yS_y + |\mu_3|I_zS_z)$, each of duration $t_2/2$, followed by $\pm 2\pi C(|\mu_2|I_xS_x + |\mu_3|I_yS_y + |\mu_1|I_zS_z)$, $\pm 2\pi C(|\mu_3|I_xS_x + |\mu_2|I_yS_y + |\mu_1|I_zS_z)$, each of duration $t_3/2$. Observe that $t_1 + t_2 + t_3 = t$ and for the optimal sequence $t_1 = t_2$ and $\frac{tan(\pi Cm)}{tan(\pi Cn)} = 2$, where $m = (|\mu_2| + |\mu_3|)t_2 + |\mu_1|t_1$ and $n = (|\mu_2| + |\mu_3|)(t_2 + t_3)/2 + |\mu_1|t_1$. These three relations determine t_1, t_2, and t_3 uniquely.

3. Next, we consider the transfer

$$\sqrt{2}I_xS_\alpha \rightarrow \sqrt{2}I_\alpha S_x.$$

Using the characterization of the local unitaries as described in equation (2). Consider the action of $A(t)$ in equation (2) on the operator $\sqrt{2}I_xS_\alpha$. Let $\mathfrak{s}$ denote the subspace spanned by the orthonormal basis $\{\sqrt{2}I_\alpha S_x, \sqrt{2}I_\alpha S_y, \sqrt{2}I_\alpha S_z\}$ and let P_s denote the projection onto this space. Then we obtain

$$P_s(A(t) \ \sqrt{2}I_xS_\alpha \ A^\dagger(t)) = \frac{\sin(\pi Ct\alpha) + \sin(\pi Ct\beta)}{2}.$$

Note $|P_s(A \ I_xS_\alpha \ A^\dagger)|$ is all we need to maximize, as then by a suitable local unitary K_1, we can rotate this projection onto $I_\alpha S_x$. Maximizing the above expression then gives $\alpha = \beta = \frac{|\mu_3|+|\mu_2|}{2}$. In practice we can achieve this efficiency by evolving the Hamiltonian $\pm 2\pi C(|\mu_3|I_xS_x+ |\mu_2|I_yS_y + |\mu_1|I_zS_z)$ for $\frac{t}{2}$ amount of time followed by the evolution of the Hamiltonian $\pm 2\pi C(|\mu_2|I_xS_x + |\mu_3|I_yS_y + |\mu_1|I_zS_z)$ for time $\frac{t}{2}$. Note, we have in the above discussion taken K_2 as identity transformation. In general if K_2 is not zero, starting from the initial operator I_xS_α, it will create $\sum_{pq} m_p n_q I_p.(\frac{\mathbf{1}}{2} - S_q)$, where $\sum_p m_p^2 = 1$ and $\sum_q n_q^2 = 1$. Since each of the terms $I_p.(\frac{\mathbf{1}}{2} - S_q)$, the maximum transfer efficiency to the subspace $\mathfrak{s}$ is bounded by $\sin(\frac{\pi}{2}Ct(|\mu_2| + |\mu_3|))$, the total maximum efficiency is achieved for K_2 an identity transformation.

4. The maximal efficiency for the transfer

$$I^\pm S_\alpha \rightarrow I_\alpha S^\pm.$$

is the same and can be derived as above.

5. Finally we consider the transfer

$$\frac{I^\pm}{\sqrt{2}} \rightarrow \sqrt{2}I_zS^\pm.$$

Consider the action of $A(t)$ in equation (2) on the operator I^+. We obtain that

$$
\begin{aligned}
A(t)I^+A^\dagger(t) &= +i\cos(\pi Ct\gamma)(I_zS_x\sin(\pi Ct\alpha) + iI_zS_y\sin(\pi Ct\beta)) \\
&+ \sin(\pi Ct\gamma)(S_x\sin(\pi Ct\beta) + iS_y\sin(\pi Ct\alpha))
\end{aligned}
$$

Thus $|\text{tr}(I_zS^-AI^+A^\dagger)|$ reduces to $\frac{\cos(\pi Ct\gamma)}{2}(\sin(\pi Ct\alpha) + \sin(\pi Ct\beta))$. We would like to have $\gamma = 0$ and α and β large but we know that (α,β,γ) lies in a convex cone as described in Theorem 1. Under these restrictions then, $\frac{\cos(\pi Ct\gamma)}{2}(\sin(\pi Ct\alpha) + \sin(\pi Ct\beta))$ is maximized for $\alpha = \beta$. To maximize α and β, we evolve the Hamiltonian $2\pi C(|\mu_2|I_xS_x + |\mu_3|I_yS_y + |\mu_1|I_zS_z)$ for $\frac{t_1}{2}$ units of time followed by evolution of $2\pi C(|\mu_3|I_xS_x + |\mu_2|I_yS_y + |\mu_1|I_zS_z)$ for another $\frac{t_1}{2}$ units of time. This produces an effective Hamitonian $2\pi Ct_1(\frac{|\mu_2|+|\mu_3|}{2}(I_xS_x + I_yS_y) + |\mu_1|I_zS_z)$. To reduce γ, we evolve the Hamiltonian $2\pi C(|\mu_2|I_xS_x - |\mu_1|I_yS_y - |\mu_3|I_zS_z)$ followed by $2\pi C(-|\mu_1|I_xS_x + |\mu_2|I_yS_y - |\mu_3|I_zS_z)$ for $\frac{t_2}{2}$ units of time each. This produces an effective Hamitonian $2\pi Ct_2(\frac{|\mu_2|-|\mu_1|}{2}(I_xS_x + I_yS_y) - |\mu_3|I_zS_z)$. Given $t_1 + t_2 = t$, we can now substitute the value of α, β and γ to find that $\cos(\pi Ct\gamma)\sin(\pi Ct\alpha)$ reduces to $\cos(\pi Ct\gamma)\sin(\frac{\pi}{2}Ct(|\mu_3| + |\mu_2| - |\mu_1| + \gamma))$. We can now maximize this expression for $|\gamma| \leq |\mu_3|$. This is the maximum efficiency. As before nothing is gained by having K_1 and K_2 other than identity transformation. The efficiency of $\frac{I^-}{\sqrt{2}} \to \sqrt{2}I_zS^-$ is the same.

References

[1] Navin Khaneja, *Geometric Control in Classical and Quantum Systems* (2000) *Ph.d. Thesis, Harvard University*).

[2] Khaneja, N., Brockett, R.W. & Glaser, S.J. (2001) *Phys. Rev. A* **63**, 032308.

[3] Glaser, S. J., Schulte-Herbrüggen, T., Sieveking, M., Schedletzky, O., Nielsen, N. C., Sørensen, O. W. & Griesinger, C. (1998) *Science.* **208**, 421-424.

[4] Burum, D. P. & Ernst, R. R. (1980) *J. Magn. Reson.* **39**, 163-168.

[5] Sattler, M., Schmidt, P., Schleucher, J., Schedletzky, O., Glaser, S. J. & Griesinger, C. (1995) *J. Magn. Reson. B* **108**, 235-242.

[6] Morris, G. A. & Freeman, R. (1979) *J. Am. Chem. Soc.* **101**, 760-762.

[7] Schleucher, J., Schwendinger, M., Sattler, M., Schmidt, P., Schedletzky, O., Glaser, S. J., Sørensen, O. W. & Griesinger, C. (1994) *J. Biomol. NMR* **4**, 301-306.

[8] Pervushin, K., Riek, R., Wider, G. & Wüthrich, K. (1997) *Proc. Natl. Acad. Sci. USA* **94**, 12366-12371.

[9] Salzmann, M., Pervushin, K., Wider, G., Senn, H. & Wüthrich, K. (1998) *Proc. Natl. Acad. Sci. USA* **95**, 13585-13590.

[10] Ernst, R. R., Bodenhausen, G. & Wokaun, A. (1987) *Principles of Nuclear Magnetic Resonance in One and Two Dimensions*, (Clarendon Press, Oxford).

[11] Glaser, S. J. (1993) *J. Magn. Reson. A* **104**, 283-301.

[12] Schulte-Herbrüggen, T., Mádi, Z. L., Sørensen, O. W. & Ernst, R. R. (1991) *Mol. Phys.* **72**, 847-871.

[13] Lieb, E. H., Schultz, T. & Mattis, D. C. (1961) *Ann. Phys.* **16**, 407-466.

[14] Tjandra, N. & Bax, A. (1997) *Science* **278**, 1111-1114.

[15] Kramer, F. & Glaser, S. J. (2002) *J. Magn. Reson.* **155**, 83-91.

[16] Hansen, M. R., Hanson, P. & Pardi, A. (2000) *Methods Enzymol.* **317**, 220-240.

[17] Gullion, T., Baker, D. B. & Conradi, M. S. (1990) *J. Magn. Reson.* **89**, 479-484.

[18] Lizak, M. J., Gullion, T. & Conradi, M. S. (1991) *J. Magn. Reson.* **91**, 254260.

[19] Kramer, F., Peti, W., Griesinger, C. & Glaser, S. J. (2001) *J. Magn. Reson.* **149**, 58-66.

[20] Weitekamp, D. P., Garbow, J. R. & Pines, A. (1982) *J. Chem. Phys.* **77**, 2870-2883.

[21] Caravatti, P., Braunschweiler, L. & Ernst, R. R. (1983) *Chem. Phys. Lett.* **100**, 305-310.

[22] Glaser, S. J. & Quant, J. J.6 (199) *in Advances in Magnetic and Optical Resonance*, W. S. Warren, Ed. (Academic Press, San Diego) **19**, 59-252.

[23] Sørensen, O. W. (1989) *Prog. NMR Spectrosc.* **21**, 503-569.

[24] Untidt, T. S. & Nielsen, N. C. (2000) *J. Chem. Phys.* **113**, 8464-8471.

[25] Khaneja, N., Reiss, T., Luy, B. & Glaser, S. J. (2003) *J. Magn. Reson.* **162**, 311-319.

[26] Stefanatos, D., Khaneja, N. & Glaser, S. J. (2004) *Phys. Rev. A* **69**, 022319.

[27] Khaneja, N. Luy, B. & Glaser, S. J. (2003) *Proc. Natl. Acad. Sci. USA* **100**, 13162-13166.